

RESEARCH

Open Access



Network efficiency of functional brain connectomes altered in type 2 diabetes patients with and without mild cognitive impairment

Juan Li^{1†}, Qiang Zhang^{2†}, Juan Wang¹, Ying Xiong^{1*} and Wenzhen Zhu¹

Abstract

Aim To explore the topological organization alterations of functional connectomes in type 2 diabetes (T2DM) patients with and without mild cognitive impairment (MCI), and compare these with structural connectomes changes.

Methods Twenty-six T2DM patients with MCI (DM-MCI), 26 without cognitive impairment (DM-NC), and 28 healthy controls were included. Diffusion tensor imaging (DTI) and resting-state functional MRI images were acquired. Networks were constructed and graph-theory based network measurements were calculated. The global network parameters and nodal efficiencies were compared across the three groups using one-way ANOVA and a false-discovery rate correction was applied for multiple comparisons. Partial correlation analyses were performed to investigate relationships between network parameters, cognitive performance and clinical variables.

Results In the structural connectome, the DM-MCI group exhibited significantly decreased global efficiency (E_{glob}) and local efficiency (E_{loc}) compared to the DM-NC and control groups. In the functional connectome, the DM-MCI group exhibited increased E_{loc} and clustering coefficient (C_p) compared to the controls. No significant differences were found in E_{glob} , E_{loc} , or C_p between the DM-NC and the control group, both in structural and functional connectomes. Nodal efficiencies decreased in some brain regions of structural and functional networks in the DM-MCI and DM-NC groups, but increased in five regions in functional network, some of which were involved in the default-mode network.

Conclusion Unlike the consistently decreased global properties and nodal efficiencies in the structural connectome of T2DM patients, increases in E_{loc} , C_p , and nodal efficiencies in the functional connectome may be viewed as a compensatory mechanism due to functional plasticity and reorganization. Altered nodal efficiency can hint at cognitive decrements at an early stage in T2DM patients.

Keywords T2DM, Mild cognitive impairment, Structural network, Functional network, Topological properties

[†]Juan Li and Qiang Zhang contributed equally to this work.

*Correspondence:
Ying Xiong
yxiong02@126.com

¹Department of Radiology, Tongji Hospital, Tongji Medical College, Huazhong University of Science and Technology, Wuhan 430030, China

²Department of Neurology, Tongji Hospital, Tongji Medical College, Huazhong University of Science and Technology, Wuhan 430030, China



Introduction

Type 2 diabetes mellitus (T2DM) can affect multiple organs and tissues, including the heart, eyes, kidneys, vasculature, and peripheral nerves, as a result of prolonged hyperglycemia [1]. Complications such as brain alterations have attracted intense attention due to their increasing prevalence. The first clinical manifestation of diabetic encephalopathy is concealed cognitive impairment. As the disease progresses, T2DM is associated with a heightened risk of developing dementia by up to 50% [2] and has been observed to correlate with a range of cognitive dysfunctions, including compromised attention, processing speed, motor skills, executive functions, and verbal memory [3], all of which can significantly diminish the quality of life. Therefore, recognizing early changes in the brain associated with diabetic encephalopathy is essential for comprehending the underlying pathophysiological mechanisms. Moreover, such recognition could be instrumental in devising early intervention strategies aimed at forestalling the onset of dementia and mitigating the progression of the disease.

The most common approaches for assessing the cognitive function of patients with T2DM remain neuropsychological tests such as the Montreal Cognitive Assessment (MoCA) and the Mini-Mental State Examination (MMSE) [4]. However, when cognition decline develops to such an extent that it can be detected clinically, widespread white matter (WM) alternations usually exist and are typically irreversible because of exacerbated metabolic syndrome. Neuroimaging studies have documented T2DM-induced cerebral morphological atrophy [5, 6], reduced microstructural integrity revealed by diffusion abnormalities [7], and functional or metabolic changes [8, 9]. Recently, it has been proposed that the human brain can be topologically modeled as an integrative and complex network, referred to as a connectome. The clinical disability and cognitive deficits observed in neurological disorders can be elucidated from the perspective of the brain's topology [10, 11]. Topological organization alterations refer to the changes in the structural and functional connectivity patterns of the brain networks, including altered nodal centrality, connectivity strength and small-world architecture. These alterations can impact the information interaction within the network and are indicative of the brain's functional and structural integrity. Therefore, analyzing network topology in patients with T2DM, particularly at the earliest stage of cognition decline, is helpful for comprehending the underlying mechanism and identifying potential biomarkers for cognitive impairment.

Graph-theory based research has revealed disruptions in the topological organization of both structural and functional brain networks in individuals with T2DM [12–14]. However, it remains unclear whether there are

structural and functional network differences between T2DM patients with normal cognition and those with cognitive impairment, and how the functional network changes due to structural modifications, highlighting the importance of integrated structural and functional network investigations in patients with T2DM. In this study, we aimed to examine the alterations in the topological organization of both structural and functional connectomes among T2DM patients with and without cognitive impairment, as well as healthy controls, by employing a combination of diffusion tensor imaging (DTI) and resting-state functional MRI (rs-fMRI) with graph theoretical analysis. Furthermore, we sought to delineate the relationships between network metrics and clinical assessments. The purposes of the current study were to investigate: (1) whether structural and functional networks are already modified in T2DM patients during the stage of normal cognition; (2) the disparities in the structural and functional networks between T2DM patients with normal and impaired cognition; (3) the variations in the nature of alterations between structural and functional networks; and (4) the correlation between network metrics and clinical parameters.

Subjects

Participants

This cross-sectional study was approved by the Institutional Review Board of Tongji Medical College, Huazhong University of Science and Technology. The study subjects comprised 28 T2DM patients (52–72 years, 18 females) with mild cognitive impairment (DM-MCI), and 28 age-, sex-, and education-matched T2DM participants (51–72 years, 18 females) with normal cognition (DM-NC) who were recruited from July 2020 to December 2022. The diagnosis of T2DM was based on standard criteria from the American Diabetes Association [15]. All participants in the study were examined by qualified physicians to confirm their clinical diagnosis and ensure their suitability for inclusion in the study. All of the participants were right-handed. Family history, clinical symptoms, use of a hypoglycemic medication, and complications were all meticulously documented. Blood biochemistry, lipids, cholesterol, plasma glucose, glycosylated hemoglobinA1c (HbA1c), and body mass index (BMI) measurements were all carefully performed. Additionally, 28 healthy volunteers (50–70 years, 18 females) without a family history of diabetes, who had fasting glucose under 7.0 mmol/L and a HbA1c level under 6.0%, were enrolled from the general population as the healthy control (HC) group. The exclusion criteria included lesions in the brain, such as cerebral infarction, hemorrhage, tumors, or vascular malformation; history of stroke, epilepsy, trauma, or brain surgery; history of

autoimmune disease or tumors; contraindication to MRI examination; and other types of diabetes.

Neuropsychological assessments

All of the participants underwent comprehensive physical, neurological, and neuropsychological assessments by qualified physicians, including the MoCA, MMSE, activity of daily living (ADL) test, Hachiski test and auditory verbal learning test (AVLT). The inclusion criteria for the DM-MCI group were as follows: (a) decline of memory started after clinical T2DM diagnosis; (b) both MoCA and MMSE scores ≤ 27 ; and (c) absence of any other physical or mental conditions that might cause cognitive impairment. The inclusion criteria for the DM-NC group were as follows: (a) no complaints of memory decline, as confirmed by family members; and (b) both MoCA and MMSE scores ≥ 27 . The Hachiski test was performed to rule out vascular dementia ($n=0$).

Materials and methods

MRI data acquisition

Images were acquired on a 3-Tesla MRI scanner (Discovery MR750, GE Healthcare, Waukesha, WI, USA) equipped with a 32-channel head coil. High-resolution anatomical images were obtained using sagittal 3D T1-weighted brain-volume imaging (BRAVO) sequence (TR/TE/TI=8.2/3.2/450 ms, slice thickness=1 mm, matrix size=256×256×160, FOV=25.6×25.6 cm², and NEX=1) to exclude possible lesions specified in the exclusion criteria. DTI data were acquired using a single-shot diffusion-weighted echo planar imaging sequence. Parameters are as follows: TR/TE=8500/66.3 ms, FOV=25.6×25.6 cm², matrix size=128×128, slice thickness=2 mm, number of slices=70, 64 diffusion gradient directions, b-value=1000 s/mm². Functional MRI images were acquired axially using a gradient-echo echo planar imaging sequence with the following parameters: TR=2000 ms, TE=35.0 ms, FOV=24.0×24.0 cm², matrix size=64×64, slice thickness=4.0 mm without spacing, acquisition bandwidth=250 kHz, and flip angle=90°. In total, 240 volumes were acquired interleaved from head to foot, with a scan time of 8 min.

Data preprocessing

The preprocessing procedures of DTI data included data conversion from DICOM to NIFTI, brain extraction, realignment, corrections of eddy current and head motion, reconstruction of diffusion tensor (fractional anisotropy, mean diffusivity, and eigenvalues) and tractography. The Pipeline for Analyzing Brain Diffusion Images (PANDA) toolbox [16] based on the FMRIB Software Library (version 5.0, <http://fsl.fmrib.ox.ac.uk/fsl/fslwiki/>) was used to carry out these processes. The following rs-fMRI data preprocessing steps were conducted

with the Data Processing & Analysis of Brain Imaging toolkit DPABI [17] (v3.0, www.nitrc.org/projects) and SPM12 (www.fil.ion.ucl.ac.uk/spm) software: the first 10 volumes were removed, taking into account the magnetization equilibrium; slice timing, head motion correction, and brain extraction were performed; then, a detrending procedure was performed to remove linear trends from the image time series, and the data were filtered at the 0.01–0.1-Hz band to remove the effects of low-frequency drift and high-frequency noise. Two subjects in the DM-MCI group and two subjects in the DM-NC group were excluded after eddy current and motion corrections (unqualified head motion).

Brain network construction

Structural connectome: The 90 (45 for each hemisphere) regions of interest (ROIs) from the Automated Anatomical Labeling (AAL) template [18] were defined as network nodes. Diffusion MRI tractography was performed using the Diffusion Toolkit software (<http://www.trackvis.org/dtk/>) with a standard method. The detailed procedures have been described in a previous study [12]. Then, a fiber-number-weighted 90×90 structural connectivity matrix was constructed for each participant. To ensure the consistency of the brain parcellation maps, all rs-fMRI images were co-registered with the b0 images, with which the individual T1-weighted images were also co-registered in the DTI space. **Functional connectome:** Based on the brain parcellation map and co-registered rs-fMRI images, the mean rs-fMRI time series was calculated by averaging over the time series of all voxels within each ROI. To measure the inter-regional resting-state functional connectivity, the Pearson correlation coefficient of the mean time series between every pair of ROIs was calculated and the corresponding significance levels were estimated. A $p < 0.05$ threshold was applied with Bonferroni correction. A weighted 90×90 functional connectivity matrix was constructed (Fig. 1). The procedures were performed using the DPABI software (v3.0, www.nitrc.org/projects).

Network analysis

Next, we analyzed the global network metrics, including global efficiency (E_{glob}), local efficiency (E_{loc}), clustering coefficient (C_p), shortest path length (L_p), and small-world parameters (λ , γ , σ). The C_p is a measure of local network connectivity and quantifies the extent that neighboring brain regions are connected. A network with a high C_p contains densely connected local clusters. E_{loc} is closely related to C_p , it reflects the average efficiency of local clusters. The L_p is a measure of global network connectivity and represents the shortest average number of connections between any two brain regions. A network is considered highly efficient if the L_p is relatively

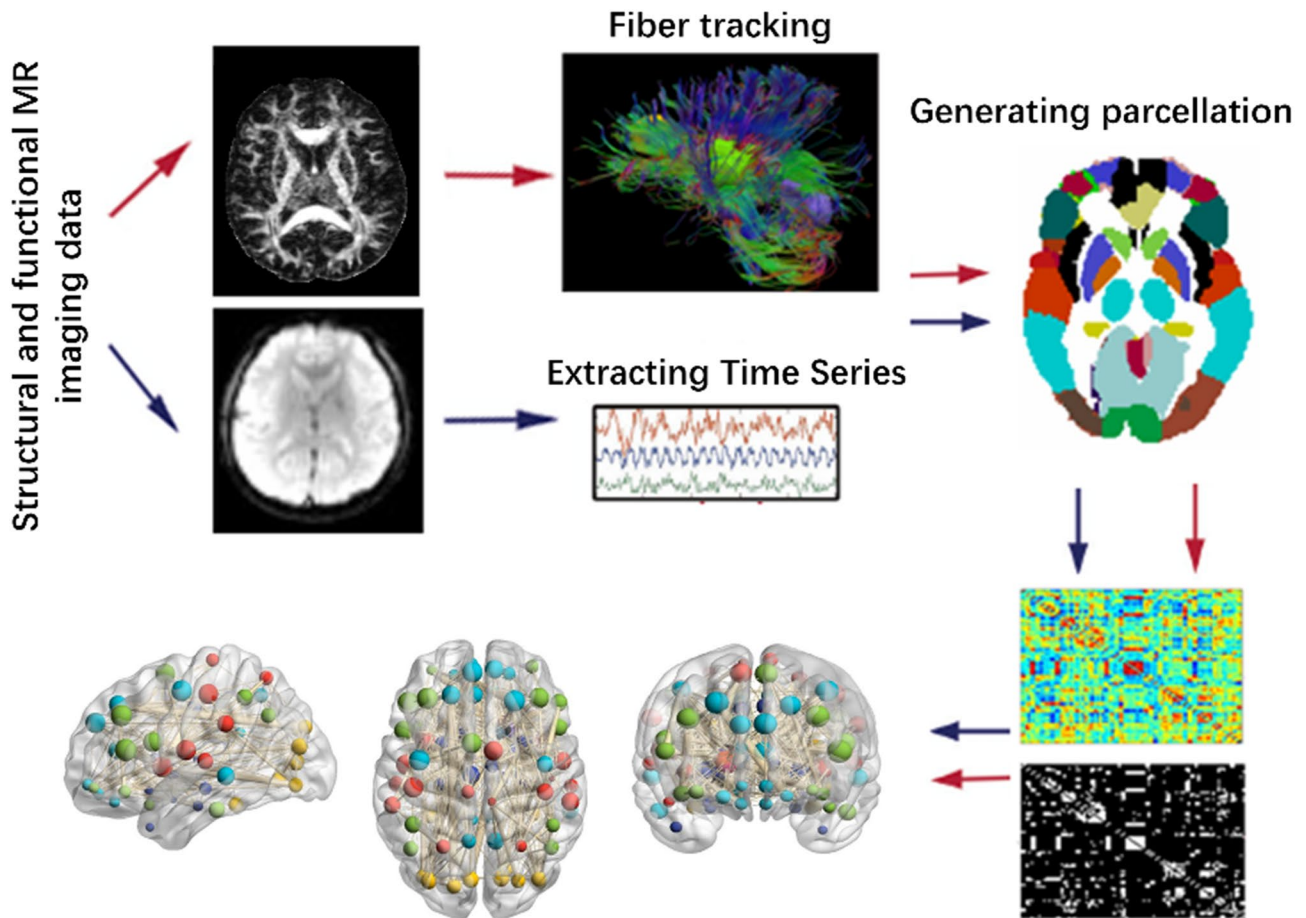


Fig. 1 Flowchart of construction of the structural and functional networks. The 90 (45 for each hemisphere) regions of interest (ROI) from the automated anatomical labeling (AAL) template were defined as the network nodes. The deterministic tractography method was applied to the diffusion MRI data to reconstruct the fiber pathways between the 90 ROIs in the brain. Functional connectivity between every two nodes was computed by extracting the rs-fMRI time series and calculating the correlation between the two nodes. The weighted and binary networks were created. The connection matrix and 3D-dimensional representation of the structural and functional networks are shown schematically

short, and this is reflected (also inversely related) in the graph measure E_{glob} [13]. To determine the regional characteristics of the structural and functional networks, we also computed the nodal efficiency in patients with T2DM and controls. When calculating these metrics of the functional network, the area under the curve (AUC) was calculated [19–21], which was sensitive at detecting topological alterations and provided a summarized scalar for the characterization (the AUCs were calculated for each parameter over the entire sparsity range in this study [$0.1 \leq Sp \leq 0.34$]). The network analyses were performed and visualized using GREYNA [22] and BrainNet Viewer [23] software. The flowchart of structural network construction is shown in Fig. 1.

Statistical analysis

Differences in demographic and clinical data were compared using SPSS 22.0 (IBM, Armonk, NY) software by a two-tailed Student's *t*-test, one-way analysis of variance

(ANOVA), or Pearson's chi-squared test, as appropriate. Differences in topologic network parameters among the three groups were analyzed using a general linear model. Age and sex were included as covariates. The global network parameters and nodal efficiencies were compared across the three groups using one-way ANOVA with a statistical significance set at $p < 0.05$; a false-discovery rate (FDR) correction was employed for multiple comparisons for nodal properties. Partial correlation analyses were applied to explore the relationship between different clinical and network measurements. Age and sex were included as covariates in the partial correlation analysis. The correlation coefficient *R* and *p*-values were calculated with a statistical significance level set at $p < 0.05$.

Results

Demographic characteristics

No group difference was noted in age or sex among the three groups. The DM-MCI group exhibited lower

MMSE and MoCA scores than the controls and the DM-NC group ($p < 0.001$). The DM-MCI group had a higher level of HbA1c ($7.9 \pm 1.5\%$) and longer duration (8.5 ± 7.4 years) than the DM-NC group ($7.0 \pm 1.3\%$, $p = 0.022$ and 4.9 ± 4.4 years, $p = 0.044$, accordingly). Details for other demographic and clinical characteristics were documented in Table 1.

Global network properties

Both the structural and functional networks of the three groups showed prominent small-world properties ($\lambda \approx 1$, $\gamma > 1$, and $\sigma > 1$). No significant intergroup differences in economical small-world organization between any two of

the DM-MCI, DM-NC and control groups were detected ($p > 0.05$). In the structural connectome, the DM-MCI group exhibited significantly decreased E_{glob} ($p = 0.003$ and 0.015) and E_{loc} ($p = 0.012$ and 0.039) values compared to the controls and DM-NC group, as well as increased Lp ($p = 0.009$) values compared to the controls. However, in the functional connectome, the DM-MCI group exhibited significantly increased E_{loc} ($p = 0.043$) and Cp ($p = 0.029$) values compared to the controls. No significant differences in E_{glob} , E_{loc} , Cp, or Lp, for both structural and functional networks, were found in the DM-NC group compared to the controls (Fig. 2).

Group differences in nodal efficiency

Significant group differences in nodal efficiency ($p < 0.05$, FDR corrected) were found in several regions for the functional network, as distributed in the frontal, parietal, temporal, and occipital cortices. In the DM-MCI group, the nodal efficiency was found to be reduced at four nodes compared to that in the controls, restricted to the left supramarginal gyrus (SMG.L), hippocampus (HIP.L), the right superior occipital gyrus (SOG.R), and fusiform gyrus (FFG.R), as well as reduced at three nodes compared to that in the DM-NC group, located in the right inferior temporal gyrus (ITG.R), FFG.R, and the left median cingulate and paracingulate gyri (DCG.L). The DM-NC group exhibited reduced nodal efficiency in the left middle occipital gyrus (MOG.L) and SOG.R compared to the controls. Further, increased nodal efficiency was found in the regions located in the left postcentral gyrus (PoCG.L) and middle temporal gyrus (MTG.L) of the DM-MCI group compared to the controls and in the left PoCG.L and MOG.L compared to the DM-NC group. Increased nodal efficiency in the HIP.L and ITG.L was found in the DM-NC group compared to the controls (Fig. 3). Intergroup differences in nodal efficiency for the structural network, which had partially been documented in detail in our previous study, were presented in Supplementary Figure.

Correlations between network metrics and clinical measurements

In the structural network of all patients with T2DM, the diabetes durations were negatively correlated with the E_{glob} ($R = -0.411$), and positively correlated with Cp ($R = 0.395$). Increased HbA1c levels were correlated with Lp ($R = 0.433$), while MMSE scores were positively correlated with lambda (λ , $R = 0.448$). In the functional network, the small world properties (lambda and sigma, λ and σ) were correlated with diabetes duration and HbA1c levels ($R = -0.372$ and 0.420 , respectively). HbA1c levels also correlated with Lp and E_{glob} ($R = -0.507$ and $R = 0.479$, all $p < 0.05$, age and sex as covariates) (Fig. 4).

Table 1 Demographic and clinical data of the participants

Clinical information	DM-MCI (n=26)	DM-NC (n=26)	HC (n=28)	$\chi^2/F/T$ value	p-value ^a
Sex (female: male)	18:8	18:8	18:10	0.203	0.904 [#]
Age (years)	61.7 ± 5.7	58.6 ± 5.9	59.9 ± 6.0	1.877	0.167 [†]
Formal education (years)	10.9 ± 3.4	11.6 ± 3.3	11.5 ± 2.7	0.295	0.746 [†]
Hypertension ^b	5 (19.2)	3 (11.5)	4 (14.3)	0.667	0.797 [#]
Hyperlipidemia ^c	4 (15.4)	2 (7.7)	4 (14.3)	0.897	0.761 [#]
Body-mass index (kg/m ²)	23.5 ± 2.6	22.7 ± 2.4	24.0 ± 1.9	2.522	0.087 [†]
Diabetes duration (years)	8.5 ± 7.4	4.9 ± 4.4	-	2.235	0.044
Insulin ever treated	3 (11.5)	1 (3.8)	-	0.271	0.603 [#]
Family history ^d	5 (19.2)	8 (30.8)	-	0.923	0.337 [#]
Complication (peripheral nerve and vascular lesions; retinopathy)	4 (15.4)	1 (3.8)	-	0.885	0.347 [#]
HbA1c (%)	7.9 ± 1.5	7.0 ± 1.3	5.3 ± 0.4	2.367	0.022
Fasting glucose (mmol/L)	10.0 ± 2.2	10.4 ± 3.3	5.29 ± 0.75	-0.552	0.583
Post-prandial glucose (mmol/L)	13.9 ± 4.4	15.4 ± 4.5	8.1 ± 1.0	-1.230	0.224
MoCA	25.3 ± 1.2	28.1 ± 0.7	28.7 ± 1.1	-10.57	< 0.001
MMSE	25.6 ± 1.9	28.5 ± 1.0	28.5 ± 1.0	-7.109	< 0.001
AVLT	30.3 ± 7.9	35.6 ± 9.3	37.8 ± 8.1	-2.096	0.043
Hachiski	1.9 ± 0.93	2.0 ± 1.03	0.67 ± 0.57	-0.421	0.676
ADL (Barthel index)	99.6 ± 1.3	99.5 ± 2.5	100 ± 0	0.627	0.839 [†]

Data are expressed as the mean ± standard deviation or percentage (%)

^ap-values labeled with [#] were obtained using a Pearson chi-squared test (two-sided), and those labeled with [†] were obtained using an ANOVA test. Other p-values were obtained using a two-tailed Student's *t*-test between the DM-MCI and DM-NC groups

^bHypertension: systolic pressure range of 140–159 mmHg or diastolic pressure range of 90–99 mmHg. Patients with moderate and severe hypertension were excluded

^cHyperlipidemia was defined as cholesterol > 5.7 mmol/L or triglyceride > 1.7 mmol/L

^dFamily history is defined as immediate family members with T2DM within three generations

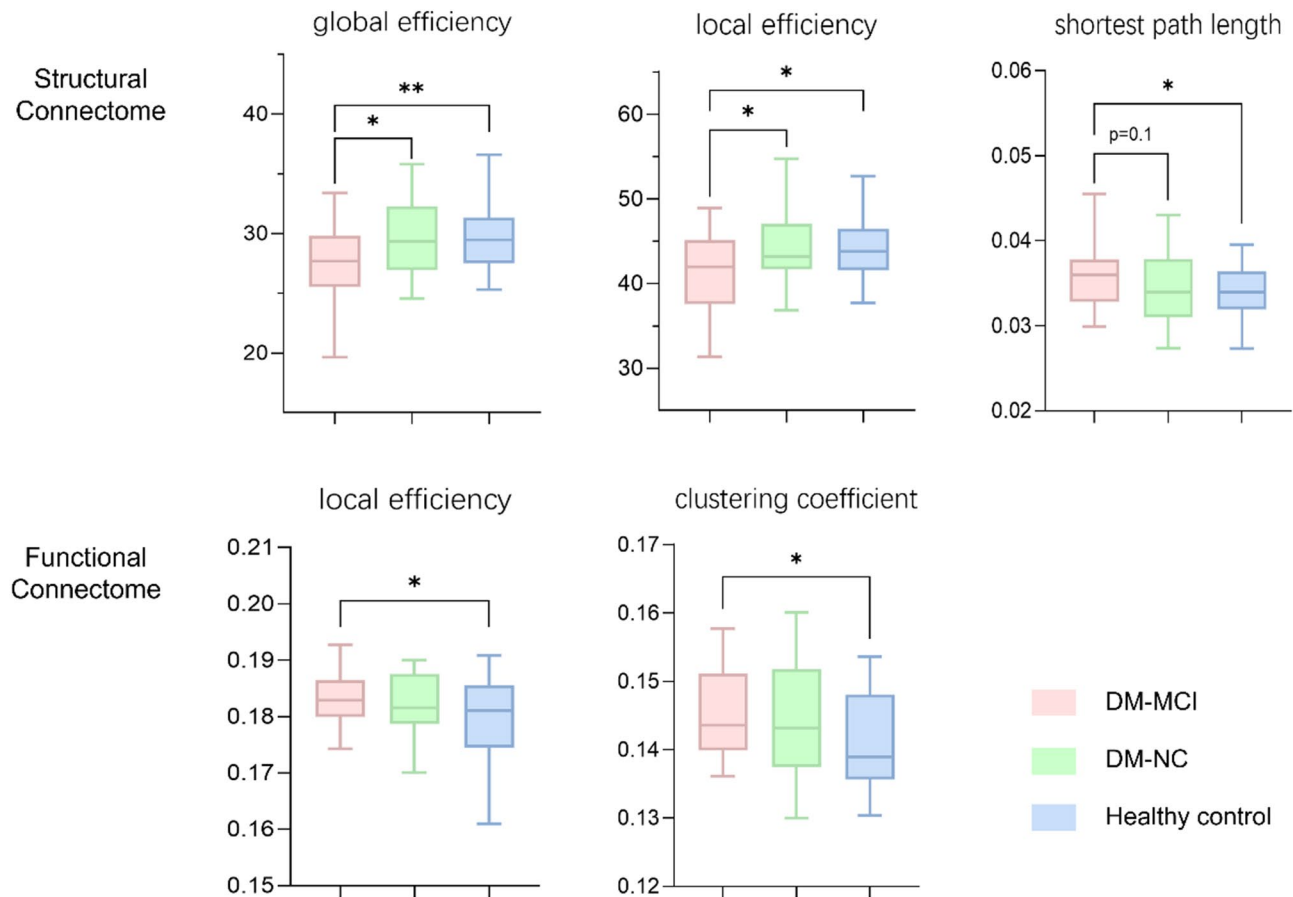


Fig. 2 Group differences in the global network metrics of the structural and functional connectomes. The bar and error bar represent the mean values and standard deviations of the network properties in each group after removing the effects of age and sex. **(A)** Significantly reduced global efficiency and local efficiency and an increased shortest path length of the structural networks were observed in the DM-MCI patients relative to both the DM-NC and controls. **(B)** Increased local efficiency and clustering coefficient of functional networks in the DM-MCI patients compared to the controls. * $p < 0.05$; ** $p < 0.01$

Furthermore, nodal efficiencies of the following brain regions were found having significant correlations with the HbA1c level (the right SMA, CAL and FFG), disease duration (the right IOG and PoCG), and neuropsychological assessments (the left PoCG and the right ITG, IPL and PAL) (Fig. 5).

Discussion

By combining DTI and rs-fMRI with graph theoretical analysis, in this study, we investigated the topological alterations of both the structural and functional connectomes in T2DM patients with and without MCI. We made several observations. First, both the structural and functional networks showed alterations in patients with T2DM, including during the normal-cognition stage. However, the network changes appeared more pronounced in the DM-MCI group compared to the DM-NC group. Second, the decreased nodal efficiencies of the structural and functional networks were detected in frontoparietal, temporal and occipital lobes, whereas

the nodal efficiencies of functional network showed increased changes in the T2DM groups within several brain regions, suggesting a possible compensatory mechanism of the functional network in the stage of cognition decline. Third, the extent of network changes was correlated with disease severity in patients with T2DM. Some previous studies [24] have also explored the topological alterations of the brain's functional network in T2DM patients using graph theory approaches. There are some differences in our study. First, we conducted a combination analysis including both the structural and functional networks within the same cohort of T2DM patients, providing a comparative analysis of the variations between them. Second, in the correlation analysis with clinical variables, we expanded the scope to include global network properties (E_{glob} , E_{loc} , C_p and L_p) as well as nodal efficiencies, with all the T2DM patients, including those with normal cognition, brought into the correlation analysis.

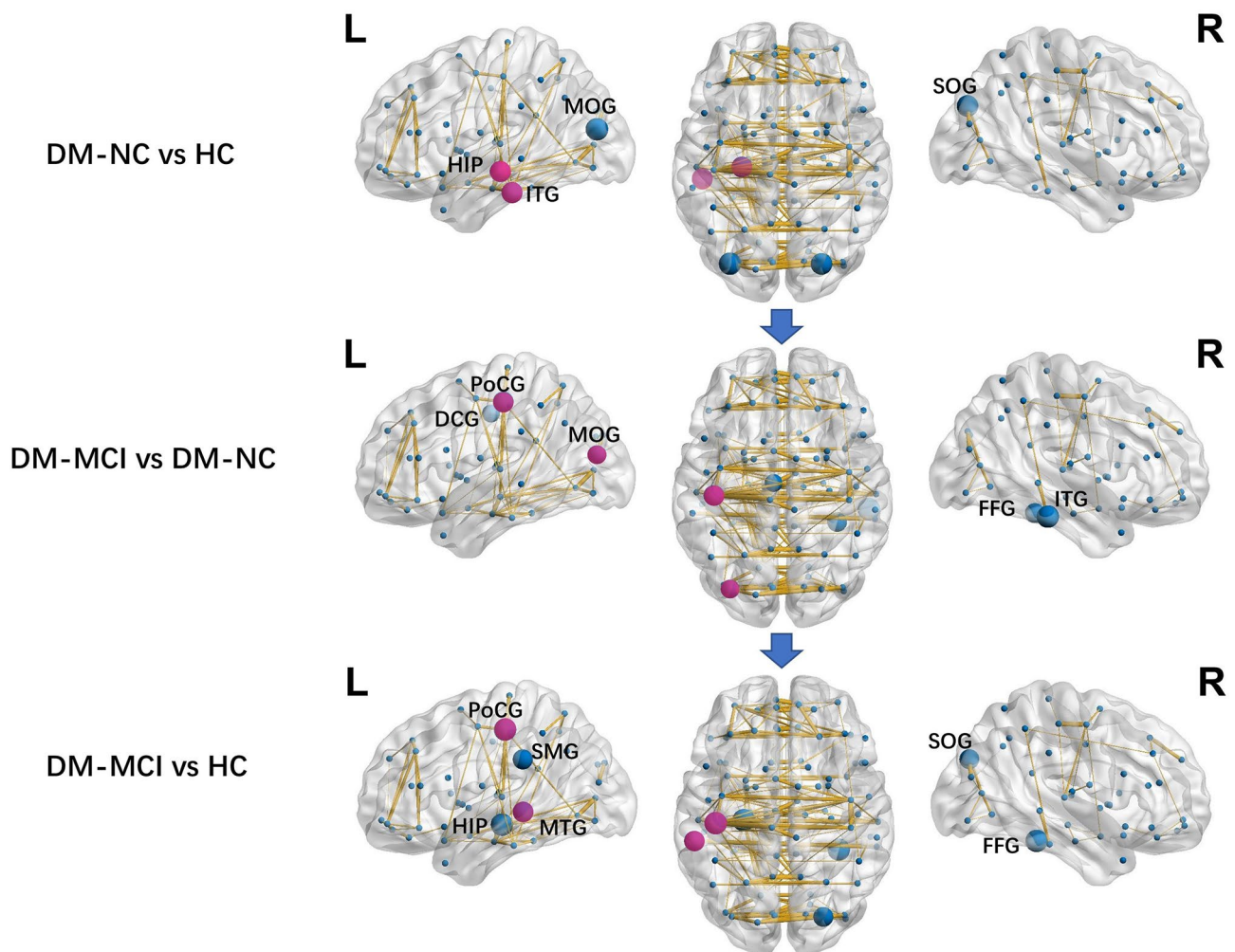


Fig. 3 Distributed brain regions with significant differences of the functional brain connectivity in nodal efficiency among the three groups. The node sizes indicate the significance of between-group differences in the nodal efficiency. The nodes in blue showed reduced efficiency in the DM-MCI and DM-NC groups compared to the controls, and decreased efficiency in the DM-MCI group compared to the DM-NC group ($p < 0.05$, corrected); the nodes in red showed increased efficiency in the DM-MCI group compared to the DM-NC and control groups ($p < 0.05$, corrected). Abbreviations: MOG: Middle occipital gyrus; HIP: Hippocampus; ITG: Inferior temporal gyrus; SOG: Superior occipital gyrus; PoCG: Postcentral gyrus; DCG: Median cingulate and paracalulate gyri; FFG: Fusiform gyrus; SMG: Supramarginal gyrus; MTG: Middle temporal gyrus

Although the small-world properties were preserved in the DM-MCI patients, some global network properties of the structural networks were significantly altered compared to the controls. The decreased E_{glob} and E_{loc} and increased L_p of the DTI networks exhibited in the DM-MCI group implied that the cognitive impairment stage of patients with T2DM was characterized by disrupted topological organization and integration in the structural connectome, underpinning changes in the functional connectome. Similar topological abnormalities in T2DM were discovered in earlier studies using graph analysis based on DTI networks [25, 26]. Furthermore, we included the DM-NC group, whose cognition status and scores were normal in clinical assessments. In these patients, the structural network properties exhibited intermediate values between the DM-MCI and

controls. In previous study we detected WM alterations in DM-NC patients [27]. We concluded that WM alterations and decreased global/local efficiency had been emerging, although the between-group difference in network metrics had not reached statistical significance.

Unlike the consistent findings in the structural network by previous studies, the analyses of the functional network showed inconsistent results. Decreased E_{glob} and increased L_p measurements revealed a decreased network efficiency [28]. Moreover, an increased efficiency (measured by increased E_{glob} , E_{loc} , and C_p) in the functional network has been reported in T2DM [13, 19–21]. According to our findings, the DM-MCI group showed significantly elevated E_{loc} and C_p compared to the controls. The combination of higher E_{loc} and C_p reflects high local specialization of the brain in information

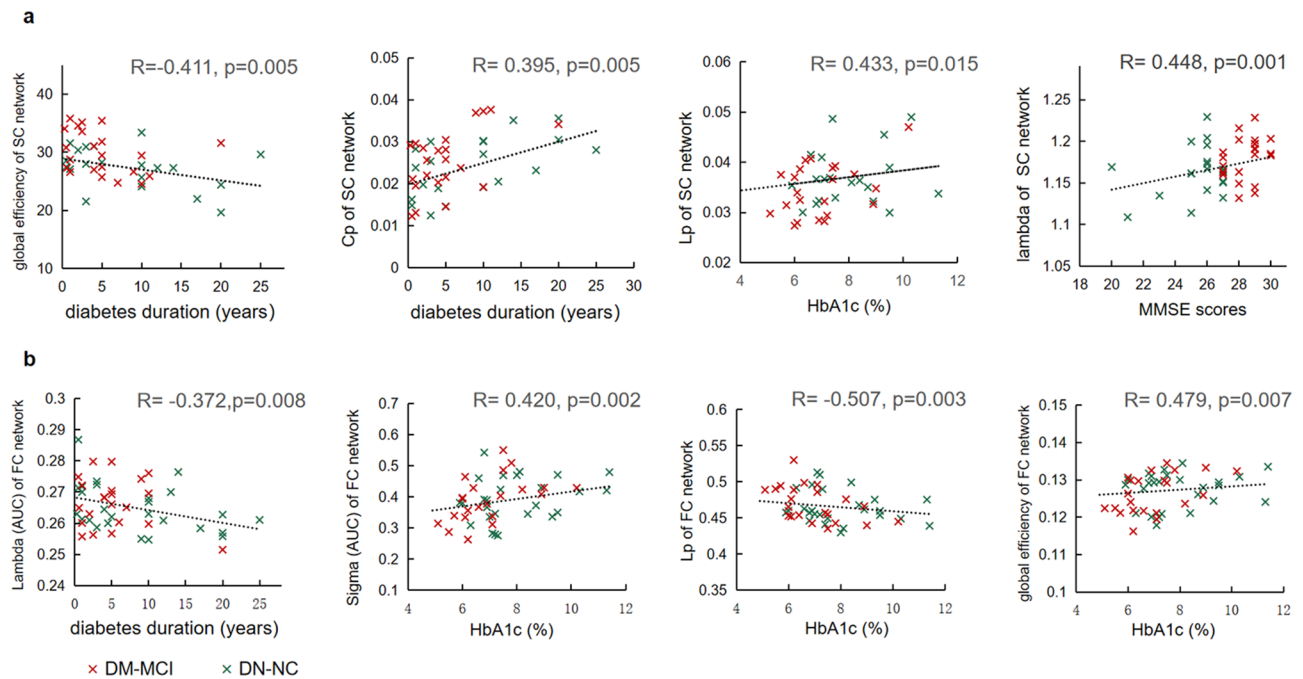


Fig. 4 Correlations between network metrics and clinical variables in patients with T2DM. Plots showing the linear correlation between the value-altered network metrics. a: Structural connectome (SC); b: Functional connectome (FC) ($p < 0.05$, R denotes Pearson's correlation coefficient with age and sex as covariates). Cp: clustering coefficient; Lp: shortest path length. MMSE: Mini-Mental State Examination

processing, as well as greater efficiency in synchronizing neuronal activity. The finding that the functional networks were “better” organized in T2DM than controls is not unique [13, 19–21]. This suggests a compensatory mechanism of the whole-brain functional network during the stage of cognition decline, which was associated with functional plasticity and increased connections.

In addition to the global network metrics, the analyses of nodal properties also provided some insights, particularly between DM-NC and controls, where the global network properties did not exhibit a significant difference. Decreased nodal efficiencies in the structural network were observed in brain regions, such as the middle frontal gyrus and posterior cingulate gyrus, which were part of the default-mode network (DMN) and may involve cognitive functions [29]. The reduced nodal efficiency may assist with the early identification of T2DM-related MCI before it is reflected by neuropsychological assessments. In contrast to the continually decreased nodal efficiencies in the structural network, in the functional network, some regions with increased nodal efficiencies were detected in both DM-NC and DM-MCI patients. We speculated that at (or even before) the emergence of clinically apparent MCI, the brain functional network may have already been reorganized as a compensatory mechanism to counteract the slight cognitive decrements.

Currently, the diagnosis of diabetes-related MCI is primarily made based on the clinical symptoms and neuropsychological tests. However, the commonly used neuropsychological scales in the clinical diagnosis of T2DM-related MCI lacks specificity and sensitivity, and is likely biased by the patient's educational background, degree of cooperation, and the subjectivity of the clinicians [30]. Therefore, biomarkers that effectively suggest the existence of MCI will help to identify and intervene at early stage of MCI, delay the occurrence of dementia, and improve the quality of life of patients with T2DM.

This study has several limitations that warrant discussion. First, the sample size was relatively moderate, which may limit generalization of the results. Second, this study was a single time-point and cross-sectional. Given the dynamic development of MCI, a longitudinal study tracking the same patients with T2DM would be better able to demonstrate the dynamic network changes to potentially predict the cognitive decline. Finally, despite finding alterations in global network metrics and nodal efficiency in some regions, it remains difficult to develop a classifier to identify an individual with MCI due to the high inter-subject variability in the network metrics and regions with altered nodal efficiency. We are enlisting more volunteers to gain a more comprehensive conclusion.

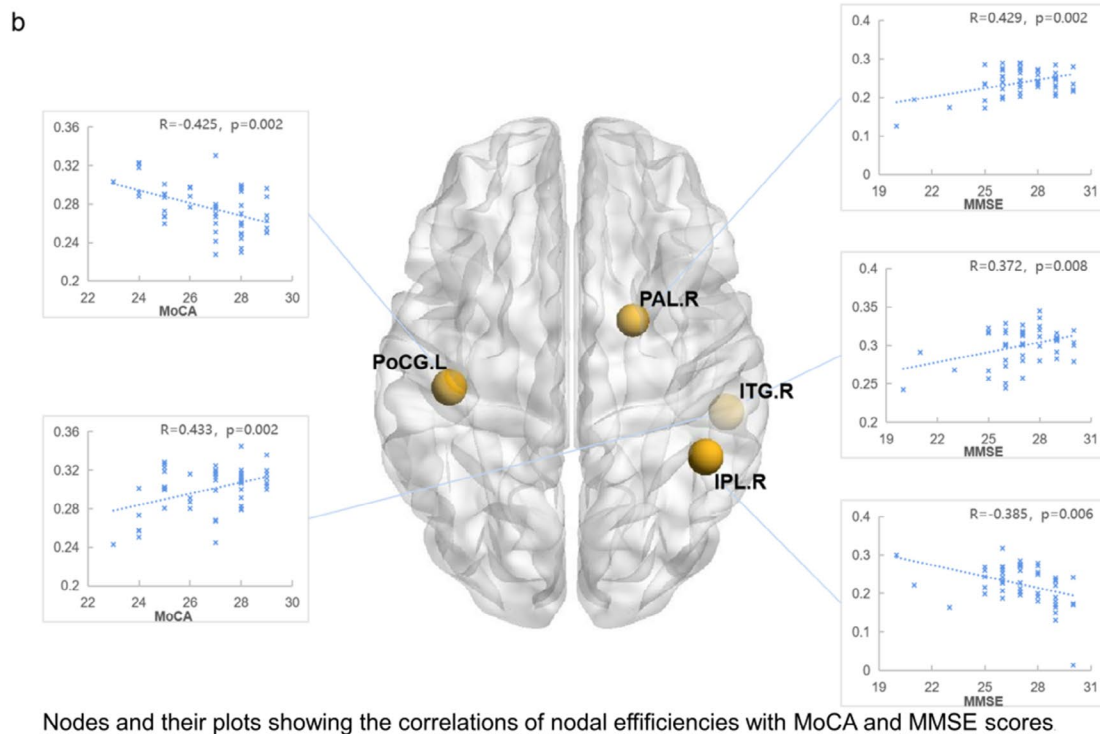
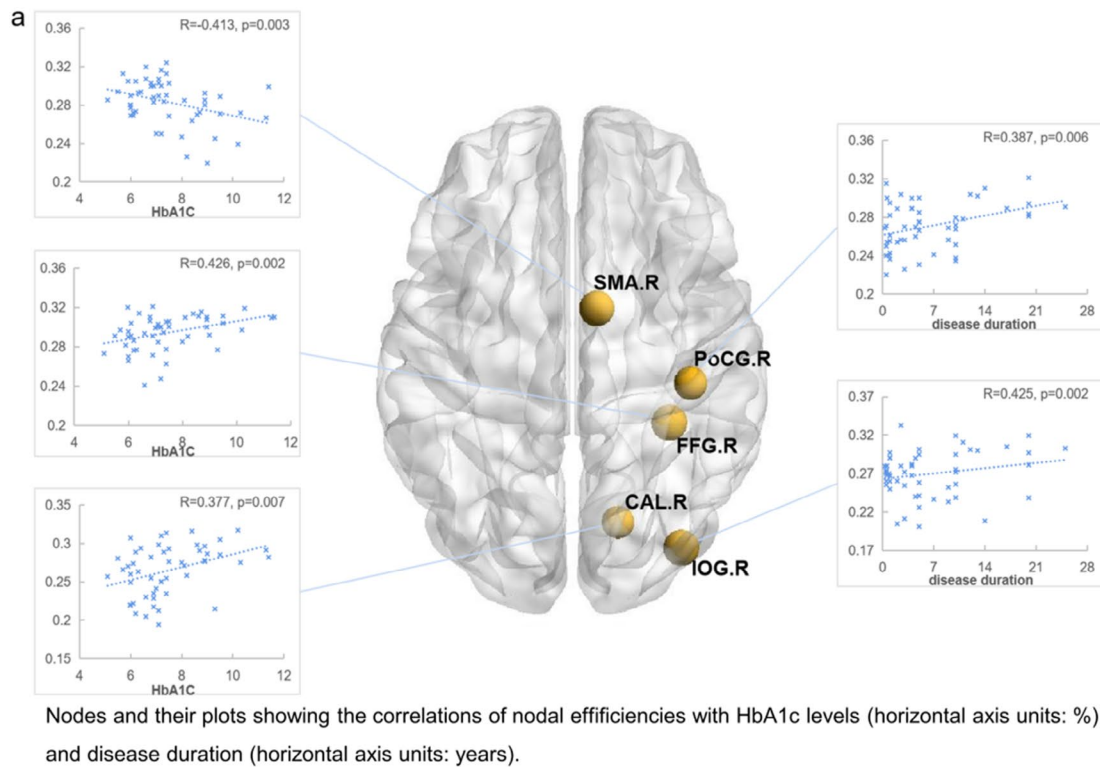


Fig. 5 Regions with significant correlations between the nodal efficiencies of functional connectome and clinical variables **(a)** HbA1c levels and disease duration; **(b)** cognitive tests scores in T2DM patients. The regions were overlaid on the brain surface at the axial view. The node sizes indicate the significance of the correlations between the nodal efficiencies and clinical variables. Abbreviations: SMA: Supplementary motor area; PoCG: Postcentral gyrus; FFG: Fusiform gyrus; CAL: Calcarine fissure and surrounding cortex; IOG: Inferior occipital gyrus; PAL: Lenticular nucleus, pallidum; ITG: Inferior temporal gyrus; IPL: Inferior parietal, but supramarginal and angular gyri. L = left; R = right. MoCA: Montreal Cognitive Assessment; MMSE: Mini-Mental State Examination

Conclusions

The disrupted topological organization of structural and functional connectomes were detected in T2DM patients with MCI or with clinically manifested normal cognition. Furthermore, network changes appeared more severe in the DM-MCI compared to the DM-NC group. We conducted combined structural and functional network studies in a T2DM patient group dataset. Unlike the consistently decreased global properties and nodal efficiencies of the structural network, the E_{loc} and C_p , as well as the nodal efficiencies in some regions (such as postcentral gyrus, inferior/middle temporal gyrus), increased in the functional network. These findings revealed that, in the process of cognition decline, the efficiency of the functional network had somewhat improved, which may have been due to a compensatory mechanism whereby the ability for local and remote information processing is enhanced due to brain functional plasticity and reorganization. The alteration of the functional connectome exhibited more complexity than the structural connectome. Altered nodal efficiency may hint at cognitive decrements in the early stage in patients with T2DM, before it is captured by neuropsychological assessments.

Supplementary Information

The online version contains supplementary material available at <https://doi.org/10.1186/s13098-024-01484-9>.

Supplementary Material 1

Acknowledgements

This work was orally presented in part at the 29th Annual Meeting of the Int'l Society of Magnetic Resonance in Medicine (Online May 15–20, 2021). The authors thank Drs. Weiyan Vivian Liu and Shiqi Yang for data collection, helpful discussions and review.

Author contributions

W.Z. and Y.X. conceived and designed the study; J.L., Q.Z. and J.W. acquired the clinical and imaging data; J.L. and Q.Z. analyzed the data and performed statistical analyses; J.L., Q.Z., J.W., Y.X. and W.Z. analyzed and interpreted the results, Y.X. wrote the main manuscript text and J.L. prepared Figs. 1, 2, 3, 4 and 5. All authors have critically reviewed the manuscript.

Funding

This work was supported by the National Natural Science Foundation of China (81601480, 82371944).

Data availability

Data will be made available to others on reasonable requests to the corresponding author. (yxiong02@126.com)

Declarations

Ethical approval

The study was conducted according to the guidelines of the Declaration of Helsinki, and was approved by the Institutional Review Board of Tongji Medical College, Huazhong University of Science and Technology.

Informed consent

Written informed consent was obtained from all participants involved in the study.

Competing interests

The authors declare no competing interests.

Received: 27 May 2024 / Accepted: 8 October 2024

Published online: 15 October 2024

References

- Zheng Y, Ley SH, Hu FB. Global aetiology and epidemiology of type 2 diabetes mellitus and its complications. *Nat Reviews Endocrinol*. 2017;14:88–98.
- Biessels GJ, Staekenborg S, Brunner E, Brayne C, Scheltens P. Risk of dementia in diabetes mellitus: a systematic review. *Lancet Neurol*. 2006;5:64–74.
- Palta P, Schneider ALC, Biessels GJ, Touradjji P, Hill-Briggs F. Magnitude of cognitive dysfunction in adults with type 2 diabetes: a Meta-analysis of six cognitive domains and the most frequently reported neuropsychological tests within domains. *J Int Neuropsychol Soc*. 2014;20:278–91.
- You Y, Liu Z, Chen Y, Xu Y, Qin J, Guo S, et al. The prevalence of mild cognitive impairment in type 2 diabetes mellitus patients: a systematic review and meta-analysis. *Acta Diabetol*. 2021;58:671–85.
- Wu G, Lin L, Zhang Q, Wu J. Brain gray matter changes in type 2 diabetes mellitus: a meta-analysis of whole-brain voxel-based morphometry study. *J Diabetes Complicat*. 2017;31:1698–703.
- Li C, Jin R, Liu K, Li Y, Zuo Z, Tong H et al. White Matter Atrophy in type 2 diabetes Mellitus patients with mild cognitive impairment. *Front NeuroSci*. 2021;14.
- Xiong Y, Sui Y, Zhang S, Zhou XJ, Yang S, Fan Y, et al. Brain microstructural alterations in type 2 diabetes: diffusion kurtosis imaging provides added value to diffusion tensor imaging. *Eur Radiol*. 2018;29:1997–2008.
- Macpherson H, Formica M, Harris E, Daly RM. Brain functional alterations in type 2 diabetes – A systematic review of fMRI studies. *Front Neuroendocr*. 2017;47:34–46.
- Del Coco L, Vergara D, De Matteis S, Mensà E, Sabbatini J, Prattichizzo F, et al. NMR-Based Metabolomic Approach Tracks potential serum biomarkers of Disease Progression in patients with type 2 diabetes Mellitus. *J Clin Med*. 2019;8:720.
- Bullmore E, Sporns O. The economy of brain network organization. *Nat Rev Neurosci*. 2012;13:336–49.
- Stam CJ, van Straaten ECW. The organization of physiological brain networks. *Clin Neurophysiol*. 2012;123:1067–87.
- Xiong Y, Tian T, Fan Y, Yang S, Xiong X, Zhang Q, et al. Diffusion Tensor Imaging reveals altered topological efficiency of structural networks in Type-2 diabetes patients with and without mild cognitive impairment. *J Magn Reson Imaging*. 2021;55:917–27.
- van Bussel FC, Backes WH, van Veenendaal TM, Hofman PA, van Boxtel MP, Schram MT, et al. Functional brain networks are altered in type 2 diabetes and prediabetes: signs for compensation of cognitive decrements? The Maastricht Study. *Diabetes*. 2016;65:2404–13.
- Chau ACM, Smith AE, Hordacre B, Kumar S, Cheung EYW, Mak HKF. A scoping review of resting-state brain functional alterations in type 2 diabetes. *Front Neuroendocr*. 2022;65:100970.
- A. AD. Diagnosis and classification of diabetes Mellitus. *Diabetes Care*. 2014;37:S81–90.
- Cui Z, Zhong S, Xu P, He Y, Gong G. PANDA: a pipeline toolbox for analyzing brain diffusion images. *Front Hum Neurosci*. 2013;7.
- Yan C-G, Wang X-D, Zuo X-N, Zang Y-F. DPABI: Data Processing & Analysis for (Resting-State) Brain Imaging. *Neuroinformatics*. 2016;14:339–51.
- Tzourio-Mazoyer N, Landeau B, Papathanassiou D, Crivello F, Etard O, Delcroix N, et al. Automated anatomical labeling of activations in SPM using a macroscopic anatomical parcellation of the MNI MRI single-subject brain. *NeuroImage*. 2002;15:273–89.
- Qin C, Liang Y, Tan X, Leng X, Lin H, Zeng H et al. Altered whole-brain functional Topological Organization and cognitive function in type 2 diabetes Mellitus patients. *Front Neurol*. 2019;10.
- Xu J, Chen F, Liu T, Wang T, Zhang J, Yuan H et al. Brain functional networks in type 2 diabetes Mellitus patients: a resting-state functional MRI study. *Front NeuroSci*. 2019;13.
- Zhang D, Huang Y, Gao J, Lei Y, Ai K, Tang M et al. Altered functional Topological Organization in Type-2 diabetes Mellitus with and without Microvascular complications. *Front NeuroSci*. 2021;15.

22. Wang J, Wang X, Xia M, Liao X, Evans A, He Y. GRETNA: a graph theoretical network analysis toolbox for imaging connectomics. *Front Hum Neurosci*. 2015;9.
23. Xia M, Wang J, He Y. BrainNet Viewer: a network visualization tool for human brain connectomics. *PLoS ONE*. 2013;8:e68910.
24. Zhou B, Wang X, Yang Q, Wu F, Tang L, Wang J et al. Topological alterations of the Brain Functional Network in type 2 diabetes Mellitus patients with and without mild cognitive impairment. *Front Aging Neurosci*. 2022;14.
25. Zhang Y, Cao Y, Xie Y, Liu L, Qin W, Lu S, et al. Altered brain structural topological properties in type 2 diabetes mellitus patients without complications. *J Diabetes*. 2019;11:129–38.
26. Zhang J, Liu Z, Li Z, Wang Y, Chen Y, Li X, et al. Disrupted White Matter Network and Cognitive decline in type 2 diabetes patients. *J Alzheimers Dis*. 2016;53:185–95.
27. Xiong Y, Sui Y, Xu Z, Zhang Q, Karaman MM, Cai K, et al. A diffusion Tensor Imaging Study on White Matter Abnormalities in patients with type 2 diabetes using tract-based spatial statistics. *Am J Neuroradiol*. 2016;37:1462–9.
28. Chen GQ, Zhang X, Xing Y, Wen D, Cui GB, Han Y. Resting-state functional magnetic resonance imaging shows altered brain network topology in type 2 diabetic patients without cognitive impairment. *Oncotarget*. 2017;8:104560–70.
29. Leech R, Sharp DJ. The role of the posterior cingulate cortex in cognition and disease. *Brain*. 2014;137:12–32.
30. Morimoto SS, Kanellopoulos D, Manning KJ, Alexopoulos GS. Diagnosis and treatment of depression and cognitive impairment in late life. *Ann N Y Acad Sci*. 2015;1345:36–46.

Publisher's note

Springer Nature remains neutral with regard to jurisdictional claims in published maps and institutional affiliations.